https://doi.org/10.48048/tis.2024.7136

Preparation and Characterization of Pelleted and Powdered Activated Carbons Derived from Used Brewed Coffee

Dewa Ngakan Ketut Putra Negara[1,2,*], I Made Widiyarta[1,2], I Made Gatot Karohika[1,2], I Gusti Agung Kade Suriadi[3], I Gusti Komang Dwijana[1], I Putu Lokantara[1], I Made Parwata[1] and I Kt Suarsana[1]

[1]Mechanical Engineering Department, Udayana University, Bukit Jimbaran, Bali 80361, Indonesia
[2]Master Program of Mechanical Engineering, Udayana University, Denpasar-Bali 80234, Indonesia
[3]Industrial Engineering Department, Udayana University, Bukit Jimbaran, Bali 80361, Indonesia

([*]Corresponding author's e-mail: devputranegara@unud.ac.id)

Received: 28 May 2023, Revised: 17 June 2023, Accepted: 27 June 2023, Published: 10 September 2023

Abstract

The experimental study is the best way to find out the characteristics of activated carbon (AC) due to its very difficult definition based on its structural formulation or chemical analysis as an effect of its high degree of imperfection in the crystal structure. This experimental study's objectives are to investigate the characteristics and the adsorption capacities of activated carbon generated from used brewed coffee. The carbonization procedure took place at a temperature of 600 °C. After being made into pellets and powder, the charcoal was heated to 600 °C and activated with the help of 150 mL of nitrogen flowing per minute. Thermogravimetric analyzer (TGA), scanning electron microscopy (SEM), and the adsorption isotherm test were all utilized in the characterization process. The results showed that for pelleted activated carbon (AC-Plt) and powdered activated carbon (AC-Pw), respectively, both activated carbons had average pore diameters in the mesopore category of 4.39 and 4.93 nm. In comparison to AC-Pw, AC-Plt has a larger specific pore surface area (105.857 cm^3/g) and pore volume (0.164 cm^3/g). The adsorption capabilities of AC-Plt, which has a bimodal pore size distribution, are greater than those of AC-Pw for nitrogen, CO_2, and methylene blue. In this investigation, it was discovered that pelleted activated carbon was more suited for the adsorption of nitrogen, CO_2, and methylene blue.

Keywords: Used brewed coffee, Activated carbon, Adsorption, Surface area, Pore size distribution

Introduction

Activated carbon is an adsorbent that can be manufactured from carbon-containing basic materials. The crystalline structure of activated carbon is uneven, with randomly scattered microcrystals. Activated carbon has a large specific surface area, a diversified pore size distribution, and a range of functional groups due to the irregularity of the nanopores structure [1]. As a result, it has a high adsorption capacity and can adsorb molecules of various substances and dimensions, allowing it to be used in a variety of applications such as CO_2 adsorption [2-4], biogas purification [5,6], supercapacitor [7,8], electrode battery [9,10], methylene blue adsorption [11,12], methane storage [13,14], water vapor adsorption [15,16], air conditioning applications [17], carbon nanotube [18-20], etc.

The demand for activated carbon is increasing due to its widespread use in many fields of life. While most activated carbon raw materials on the market are derived from wood, coal, petroleum residue, lignite, and polymers [1]. Except for wood, none of these raw materials are renewable or cheap. Various alternative raw materials, particularly those derived from biomass, have been investigated, including coconut shell [21,22], barley straw [1], sugarcane bagasse [23], bamboo [24-26], rice husk [27,28], coffee ground [29,30], palm empty fruit bunches [31], wild algae [32] and others.

The use of biomass as a raw material for activated carbon is very promising because it is plentiful and relatively inexpensive. The chemical composition of biomass, whose main components consist of cellulose, lignin, and hemicellulose, is one of the factors that determine the quality of activated carbon. Another consideration is the selection of the appropriate manufacturing parameters. Dehydration, carbonization, and activation are all steps in the production of activated carbon. Dehydration seeks to reduce the sample's water content; carbonization seeks to convert precursors into char with high fix carbon; and activation seeks to increase the porosity of the sample so that it has a high adsorption capacity.

Carbonization is usually carried out by heating the raw material in an oxygen-poor environment at a temperature of 300 - 800 °C [1]. Carbonization produces char, which has a low adsorption capacity because the pores are partially covered by other products of carbonization, especially in the form of tar. To open the pores of the tar dew, an activation process is carried out, either physical and chemical activation or a combination of the two. Physical activation is accomplished by heating at 400 - 600 °C [33] or 700 - 1000 °C [1] while simultaneously flowing oxidizing gases such as H_2O, CO_2, or air [33] or nitrogen gas [34]. While chemical activation is carried out by involving chemical agents such as K_2CO_3, H_3PO_4, $ZnCl_2$ and KOH through heating at a temperature of 400 °C [33].

Coffee is 1 type of biomass, and it is the world's 2nd most traded commodity [35]. One tone of coffee is thought to produce 650 kg of waste coffee grounds (brewed coffee), which translates to an annual production of more than 6 million tons of coffee grounds [36]. Several studies have been conducted to investigate the use of brewed coffee waste as activated carbon. Mukherjee *et al.* [29], produce powdered activated carbon from spent coffee grounds using 3 different process routes: Slow pyrolysis, CO_2 activation, and flue gas recycling for activation (Scenario 1); flue gas combustion (Scenario 2); and flue gas combustion and deep eutectic solvent impregnation (Scenario 3). Each scenario's process route evaluation is based on economic viability, such as discounted cash flow rate of return, net present value, and payback period. All of the scenarios were found to be economically viable. Hossain *et al.* [30] produce powdered activated carbon using post-consumer coffee grounds as a raw material. Carbonization was carried out at 600 °C with a nitrogen flow rate of 1 L/min, and activation using a combination of CO_2 and Ar activators at 650, 750 and 850 °C. The resulting activated carbon has a surface area varying from 23.3 to 579.9 m^2/g, pore volume of 0.068 to 0.365 cm^3/g, and an average pore diameter of 2.4 to 5.6 nm [30].

With modifications in the impregnation ratio (IR) char/KOH 1:0, 2:1, 1:1 and 2:3 and variations in the carbonization temperature (600, 700 and 800 °C) [37], brewed coffee waste is converted into activated carbon. The resulting activated carbons have pore diameter that range in size from 1.04 to 1.97 nm on average, can adsorb caffeine at a rate of 27 to 90.4 %, and operates best under conditions where the carbonization temperature is 800 °C and the IR is 1:1. Hadebe *et al.* [38], uses the hydrothermal treatment method with an activation temperature of 800 °C to manufacture chemically activated carbon from brewed coffee using KOH with an IR of 9:1 (coffee brewed: KOH, % wt). The generated activated carbon has a 323.1670 m^2/g pore surface area, 0.2607 cm^3/g pore volume, 3.716 nm pore diameter, and 145 cm^3/g nitrogen adsorption capacity. Ferraz and Yuan [39] also produce brewed coffee powder activated carbons via chemical activation (H_3PO_4) at temperatures of 350 and 500 °C with IR of 50 and 100 % wt. The activated carbons produced have pore surface area (S_{BET}) values ranging from 188 to 2,118 m^2/g, pore volumes ranging from 0.030 to 0.182 cm^3/g, and average pore diameters ranging from 2.5 to 3.8 nm, and are used for COD (chemical oxygen demand) adsorption and color removal from landfill leachate. On activated carbon, optimal conditions were obtained with an IR of 50 % and an activation temperature of 500 °C, with COD and color adsorption efficiencies of 94 ± 3 and 100 %, respectively. However, the majority of the used brewed coffee activated carbons surveyed were powdered and chemically activated, and finding one in pellet form was extremely difficult. Pelleted activated carbon, on the other hand, has an advantage in the adsorption process because of its high volumetric adsorption capacity, ease of handling, and ability to be thermally reactivated and utilized repeatedly. Furthermore, the investigation of pelleted-activated carbon characteristics obtained from physically activated used brewed coffee is an interesting research topic and a novelty in this study.

This study aims to compare the characteristics and adsorption capacities of pelleted and powdered activated carbons made from used brewed coffee. Investigated properties of the activated carbons included their proximate composition, pore surface area, volume, diameter, and surface morphology. The adsorption capacities of activated carbons include their adsorption of nitrogen, CO_2, and methylene blue. The expected contribution of this research is to be able to add information and knowledge, especially about the characteristics and adsorption capacity of activated carbon in various forms, including pelleted and powdered activated carbons.

Materials and methods

Materials and preparation of activated carbon

The precursor, Arabica-used brewed coffee, was collected from a coffee shop in Denpasar, Bali - Indonesia. Nitrogen and CO_2 were sourced from PT. Samotor Gas Industry. Control parameters applied in the preparation of activated carbon include temperature and duration of dehydration, carbonization temperature, charcoal mesh size, binder, and hydraulic pressure during the production of pelleted

activated carbon, activation temperature, and nitrogen flow rate as follows: The used brewed coffee with a 50-mesh particle size (less than 297 µm) was dried in an electric furnace at a temperature of 105 °C for 3 h, then cooled to room temperature. The dehydrated sample was then carbonized by heating it to 600 °C in an oxygen-depleted environment due to the sample was placed in the reactor with no contact with air. The detention at 600 °C lasted 50 min before being cooled for 12 h in the electric furnace. The carbonized samples were then meshed at a mesh size of 60, indicating that the grain size was less than 250 µm. A 30 g sample was left in powder form, while another 30 g sample was mixed with 10 % wt natural binder (a mix of tapioca flour and aquadest) and pressed with a hydraulic press device at pressures of 17, 18, 19, and 20 psi to produce the carbon pellet.

The activation process is carried out by inserting carbonized powder and pellet char into the reactor of a programmable tubular electric furnace, as shown in **Figure 1**. The sample is heated to 600 °C before being fed with nitrogen at a rate of 150 mL/min for 50 min, as determined by a flow mass controller. Furthermore, samples are cooled in the electric furnace for 12 h. The resulting activated carbon is denoted by the symbols AC-Plt and AC-Pw for pelleted and powdered activated carbons, respectively, as shown in **Figure 2**. Pelleted activated carbon produced with a pressure of 20 psi yields the best product with the lowest defect, having dimensions (diameter × height) of 20×13 mm^2, as shown in **Figure 2(a)** I. This pelleted activated carbon is selected as a sample to be characterized and tested for its adsorption capacity. Thus, the pressure of 20 psi becomes one of the control variables, and the independent variable in this study is only the form of activated carbon, namely pelleted and powdered activated carbon.

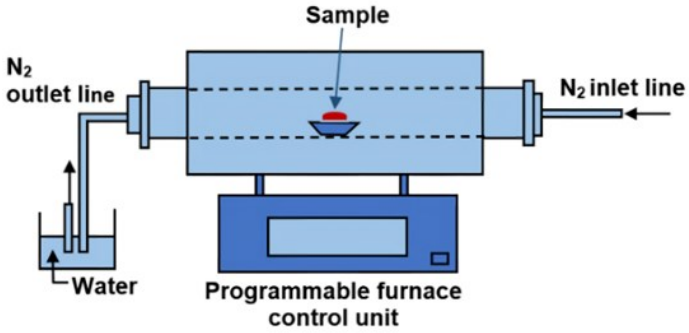

Figure 1 Schematic of programmable tubular electric furnace.

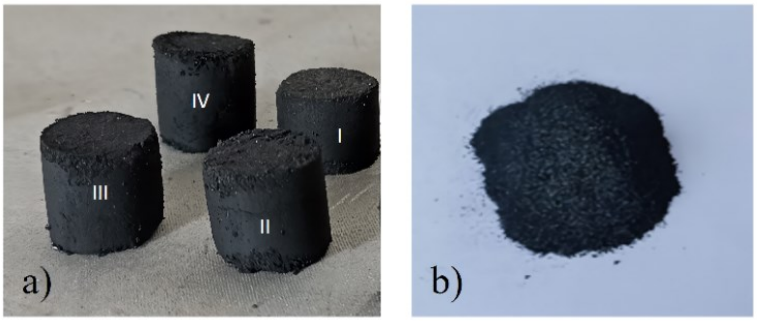

Figure 2 Activated carbons: a) Pelleted activated carbon with forming pressure 20 psi (I), 19 psi (II), 18 psi (III), and 17 Psi (IV) and b) Powdered activated carbon.

Characterization of activated carbons

The purpose of the characterization was to determine the properties and adsorption capacities of activated carbons. Proximate, SEM, adsorption isotherm, CO_2 and methylene blue adsorption tests are among those performed. The proximate test was used to determine the activated carbon's moisture, volatile, ash, and fixed carbon content using TGA 701 device, ASTM D7582 MVA Biomass. The SEM test was performed with the SEM-JSM-651OLA device to examine the surface morphology of activated carbons. The adsorption isotherm test was performed with Quantachrome Nova Instruments Version 11.0 to determine the specific pore surface area (S_{BET}), pore volume (V_P), pore diameter (D_P), and nitrogen adsorption capacity of activated carbons. S_{BET} was determined at relative pressures ranging from 0.1 - 0.3 and 0.096 to 0.304 for AC-Plt and AC-Pw, respectively.

Methylene blue and CO_2 adsorption tests

The parameters controlled in the methylene blue test include the concentration of the solution, the amount of activated carbon used, the length of the mixing process, and the time until adsorption equilibrium is reached, as follows: The methylene blue adsorption test was performed by mixing 20 mL of methylene blue at a concentration of 5 ppm with 0.1 g of activated carbon. For pelleted activated carbon, 0.1 g of sample is taken by breaking the pellets and then selecting pellet fractions with a mass of 0.1 g. To obtain a homogeneous solution, a magnetic stirrer was used for 20 min of mixing and it is left for 100 min to allow for adsorption equilibrium. The solution was then filtered through filter paper. An Ultra Violet-Visible (UV-Vis) 600 spectrometer with a wavelength of 664 nm was used to measure the concentration of the filtered filtrate. The measured concentration is the methylene blue residual concentration. The difference between the initial and the residual concentrations is the adsorbed concentration.

The gravimetric method was used to conduct the CO_2 adsorption test, as illustrated in **Figure 3**. The following parameters are controlled in this test: Degassing temperature, vacuum pressure during degassing process, and CO_2 gas pressure during the adsorption process: The sample holder was attached to the wire connected to the analytical balance, and the value is set to 0. Activated carbon was then placed in the sample holder, weighed and recorded as w_o. The glass tube is placed in a vertical tubular furnace and heated to 100 °C. Degasing is done with a vacuum pump at a pressure of 1 bar to allow the gases in the activated carbon to escape. Furthermore, the CO_2 was injected into the sample at 1 bar pressure and the mass change was measured with a digital analytical balance and recorded on a computer. When there is no further mass change, it indicates that the adsorption process has been completed and the final mass was recorded as w_t. The test was repeated 3 times both for AC-Plt and AC-Pw. The mass of CO_2 adsorbed (w_a) is the difference between w_t and w_o, and formulated as Eq. (1). The specific adsorption capacity (S_{ac}) of activated carbon was calculated by use of Eq. (2), where Mr CO_2 is the relative molecule mass of CO_2 (44 g/mol).

$$w_a = w_t - w_o \text{ (g)} \tag{1}$$

$$S_{ac} = \frac{W_a}{Mr\ CO_2 .\ w_o} \times 1000\ \left(\frac{mmol}{g}\right) \tag{2}$$

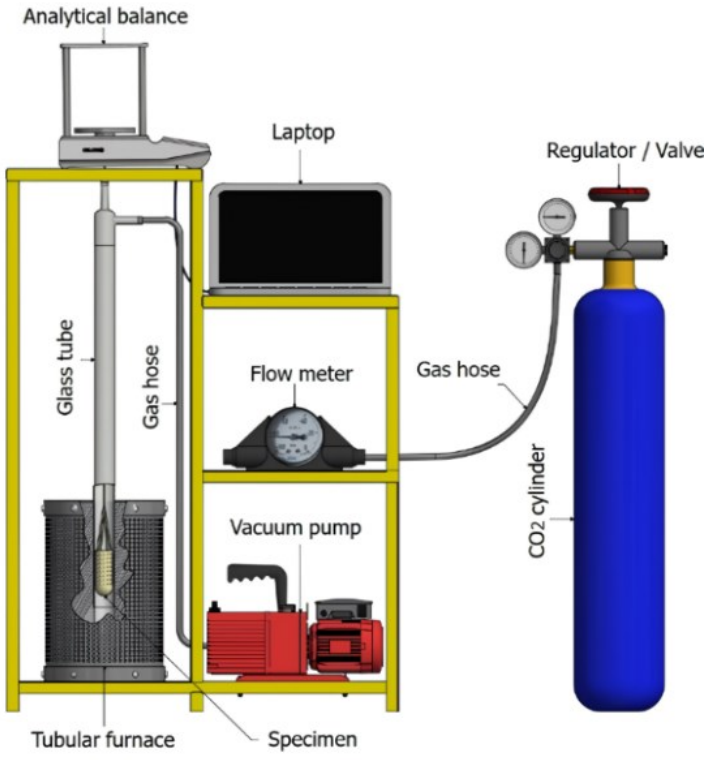

Figure 3 Schematic of gravimetric CO_2 adsorption test.

Results and discussion

TGA analysis

The TGA test results are presented in the form of a graph that shows the relationship between the mass reduction, temperature, and time of each activated carbon, as shown in **Figures 4**. **Figures 5** and **6** show a comparison of the mass changes of the 2-activated carbons with respect to time and temperature. **Table 1** shows the composition of proximate activated carbon. From **Figures 4**, it can be seen that the TGA curves of the 2-activated carbons are nearly identical, but significant mass changes occur at different temperatures and time intervals, as shown in **Figures 5** and **6**, respectively, indicating the loss of certain components in the sample also occurs at different temperatures and time intervals.

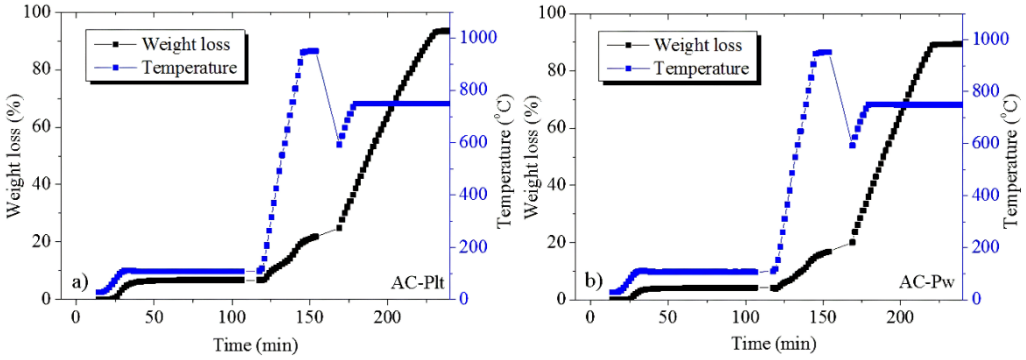

Figure 4 TGA curve of a) pelleted activated carbon (AC-Plt) and b) powdered activated carbon (AC-Pw).

Heating to 107 °C is a moisture process that dehydrates the organic matter, resulting in the desorption of free and chemically bound water from the sample. At this stage, the reduction in mass that occurs is very small. In 40 min, the mass of AC-Plt was reduced by 7 %, while the mass of AC-Pw was reduced by 3 % in 36 min. The sample mass remained constant at this temperature for 77 min for AC-Plt and 81 min for AC-Pw. Furthermore, a volatile step occurs between 107 and 950 °C. The evaporation of volatile substances in the sample resulted in a significant reduction in mass in this range temperature, resulting in an increase in the fixed carbon content in the sample. The remaining mass in this stage of AC-Plt is approximately 78 %, and the remaining mass of AC-Pw is approximately 83 %.

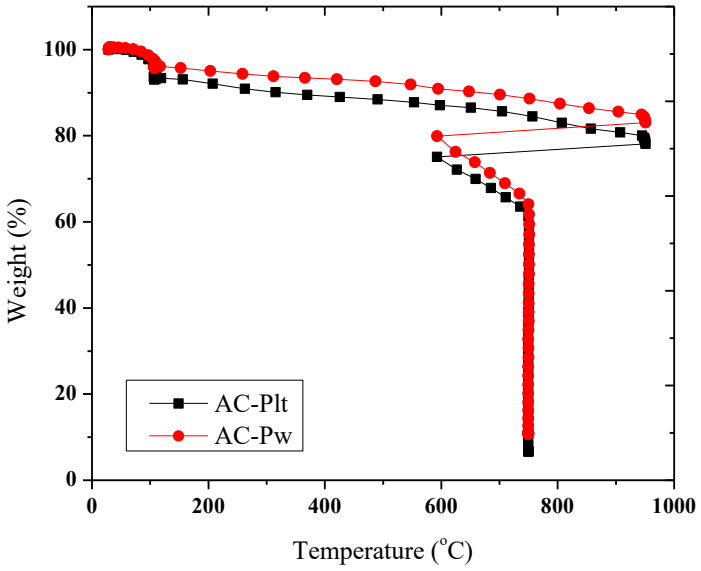

Figure 5 TGA curve (weight vs temperature) of activated carbons.

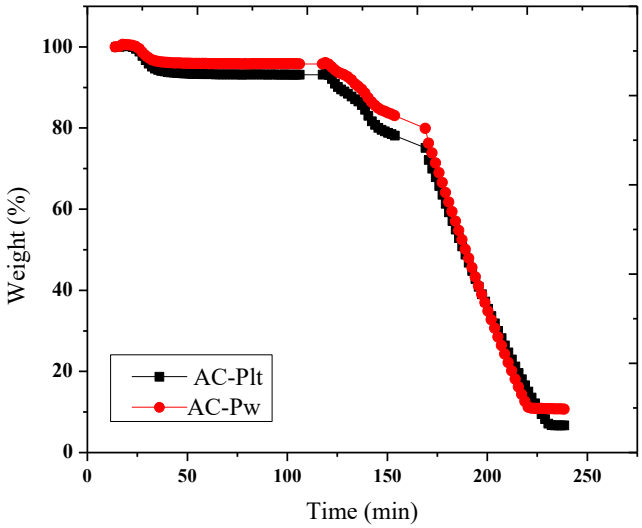

Figure 6 TGA curve (weight vs time) of activated carbons.

The test temperature was then reduced to 600 °C while the sample was simultaneously fed with oxygen, allowing the sample combustion process to take place. At temperatures ranging from 600 to 750 °C, the mass of activated carbon remaining is 61 % for AC-Plt and 64 % for AC-Plt. Ash began to form at 750 °C and remained at that temperature for approximately 40 min for AC-Plt and 50 min for AC-Pw until all samples turned to ash completely. As shown in **Figures 5** and **6**, and **Table 1**, the final mass of the sample is ash mass, which is 6.68 % for AC-Plt and 10.72 % for AC-Pw. The total time required for AC-Plt to become ash is longer than for AC-Pw because the presence of binder residues on the pellet activated carbon necessitates a longer combustion process.

According to **Table 1**, there is no activated carbon with a superior proximate composition to the others. A good composition of activated carbon has a high fix carbon content, low ash, moisture, and volatile content. AC-Pw has more fix carbon, less moisture, and less volatile than AC-Plt, but more ash. Ash is made up of metal oxides in charcoal that do not evaporate (are non-volatile) during the heating process. The high ash content can cause the activated carbon pores to clog, thereby reducing the pore surface area and resulting in a reduced adsorption capacity.

The composition of proximate AC-Plt and AC-Pw meets the requirements for activated carbon set forth in the Indonesian National Standard SNI 06-3730-1995, which states that a good activated carbon must contain a minimum of 65 % fixed carbon and a volatile, moisture, and ash content that does not exceed 25, 15 and 10 %, respectively.

Table 1 The proximate composition of activated carbons.

Activated carbons	TGA elements (%)			
	Moisture	Volatile	Ash	Fixed carbon
AC-Plt	6.60	15.21	6.68	71.51
AC-Pw	3.39	12.99	10.72	72.33

Adsorption isotherm and pore size distribution

Figure 7 shows the adsorption isotherm curve of activated carbon. The curves show a relationship that exists between the equilibrium pressure of a gas and the amount of gas adsorbed on a solid adsorbent at a constant temperature. The amount of nitrogen adsorbed until the adsorption process ceases is proportional to the increase in relative pressure. This is due to the fact that activated carbon has a finite number of pores. When the pressure is high enough, all sites are filled, and increasing the pressure has no effect on the adsorption process further. AC-Plt has a higher adsorption capacity than AC-Pw at all relative pressure levels. This is due to the fact that AC-Plt has a larger specific pore surface area and pore volume than AC-Pw, as shown in **Table 2**. At the end of the process, at a relative pressure of one, AC-Plt could absorb 75.252 cm^3/g of N_2, whereas AC-Pw could absorb 38.776 cm^3/g.

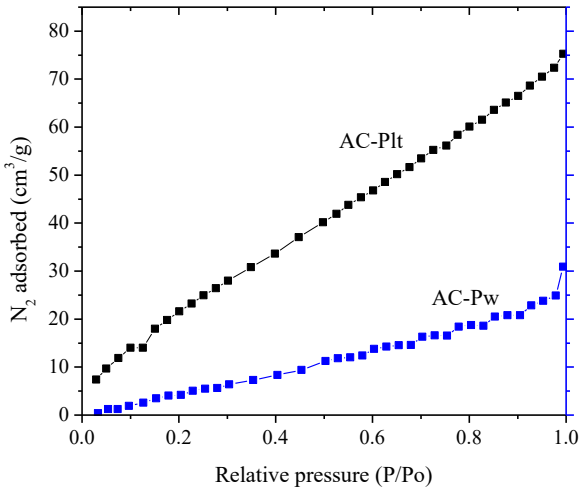

Figure 7 Adsorption isotherm of activated carbons.

Figure 8 depicts the distribution of pore sizes from activated carbons to a diameter of 30 nm. The activated carbon pore size distribution quantifies the relative pore volume associated with various pore sizes. In general, the pore size distribution is divided into a zone that is less than 2 nm (micropores zone) and a zone from 2 to 50 nm (mesopore zone). When compared to PC-Pw, AC-Plt has more micropores. Despite the fact that AC-Pw has almost no micropores, the average pore diameter of AC-Plt is smaller than that of AC-Pw. Both activated carbons have mostly mesopore pores (2 - 50 nm) that are bimodally distributed with each have 2 peaks that are also located in mesopore region. The highest peaks of activated carbon AC-Plt (0.028 $cm^3/g/nm$) and AC-Pw (0.016 $cm^3/g/nm$) occurred at pore diameters of 2.465 nm and 3.590 nm.

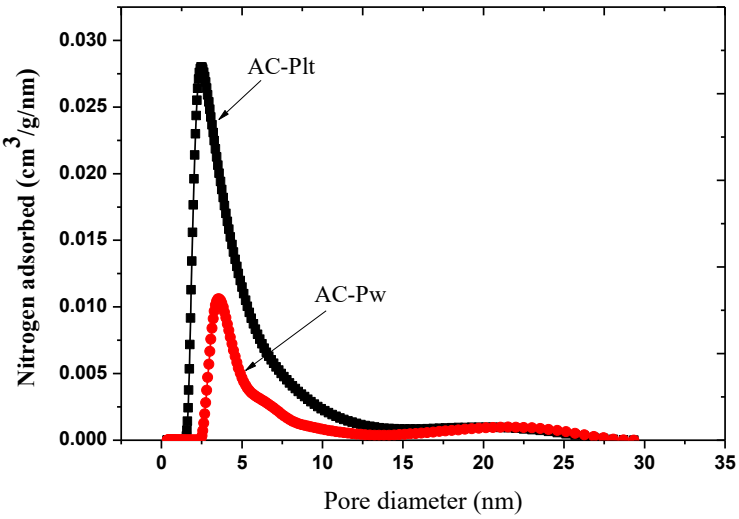

Figure 8 Pore size distribution of activated carbons.

Surface structure and morphology of activated carbons

The surface structure of activated carbons is shown in **Table 2**, including specific pore surface area (S_{BET}), specific pore volume (V_P), and average pore diameter (D_P). AC-Plt activated carbon has a higher specific pore surface area (105.857 m^2/g) and volume (0.164 cm^3/g), but the average pore diameter is smaller. The higher specific surface area and pore volume of AC-Plt are possibly because the ash content of AC-Plt is lower than that of AC-Pw, allowing only a small portion of the pores to be covered, resulting in AC-Plt having a greater surface area and pore volume than AC-Pw. Another possibility is that the

natural binder undergoes pyrolysis during the activation process, producing gas that acts as an activating agent (e.g., CO_2) so that nitrogen and CO_2 work simultaneously and more effectively to develop more activated carbon pore structures. A substance's activated carbon adsorption capacity is related to its pore surface area and pore volume. In general, the greater the pore surface area and volume, the greater a substance's ability to adsorb. The adsorption capacity, however, is also affected by the pore size distribution and the molecular dimensions of the adsorbed substance. A substance's molecular dimensions can only be adsorbed if they are equal to or smaller than the pore diameter of the activated carbon. The smaller average pore diameter of AC-Plt than AC-Pw is most likely due to the pressing process during pellet production, which causes some of the larger pores to narrow. However, additional tests, such as the XRD test, are required to determine whether the pressing process in the manufacture of pellets causes a change in the arrangement of the crystals.

Table 2 Surface structure of activated carbons.

Activated carbons	S_{BET} (m^2/g)	V_P (cm^3/g)	D_P (nm)
AC-Plt	105.857	0.164	4.39
AC-Pw	38.776	0.048	4.93

Figure 9 depicts the surface morphology of AC-Plt and AC-Pw activated carbon. The surface morphology of activated carbons is characterized by heterogeneity and irregular pore and cavitation distribution [40]. According to **Table 2** and **Figure 9**, the majority of the pore diameters are mesopores with mostly irregular pore shapes. These pores form during the carbonization and activation processes. It can be seen that the majority of the pore diameters of AC-Pw are larger than the pore diameters of AC-Plt, which is quantitatively consistent with **Table 2**. Other surface structure parameters are difficult to see in this SEM image, but they have been determined by an adsorption isotherm test, as shown in **Table 2**.

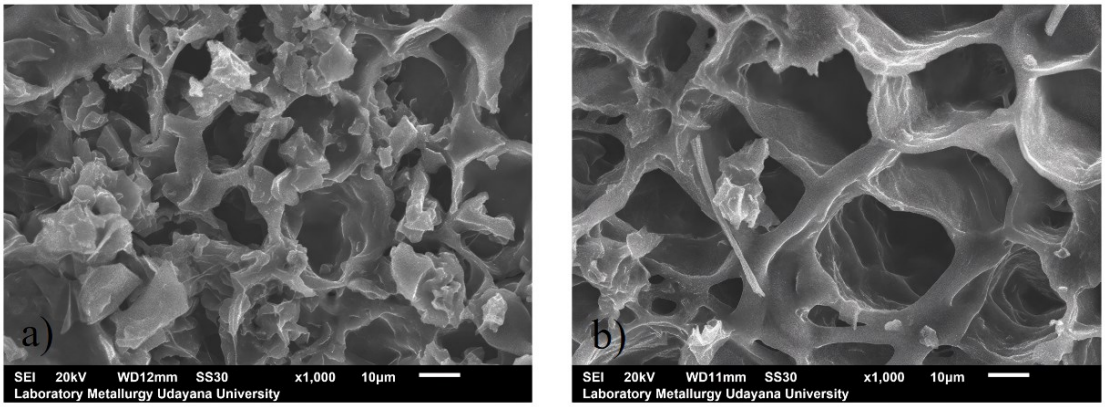

Figure 9 Surface morphology of activated carbons: a) AC-Plt and b) AC-Pw.

Adsorption of nitrogen, CO_2, and methylene blue (MB)

Table 3 shows the adsorption capacities of AC-Plt and AC-Pw activated carbon against nitrogen, CO_2, and methylene blue. AC-Plt is more capable of adsorbing nitrogen, CO_2, and methylene blue than AC-Pw due to the fact that it has a larger pore surface area and volume than AC-Pw. Furthermore, AC-Plt pores are found in both the micropore and mesopore regions, whereas AC-Pw pores are almost entirely found in the mesopore region. As a result, the 3 substances are adsorbed in the AC-Plt micro and mesopore regions but only in the AC-Pw mesopore region. As a result, more substances can be stored in AC-Plt than in AC-Pw.

According to the proximate properties of activated carbon, the ash content plays the more important role in activated carbon's adsorption capacity for nitrogen, CO_2, and methylene blue. Despite having a lower fixed carbon content than AC-Pw, AC-Plt has the highest adsorption capacity due to its lower ash content of 37.68 %. Lower ash content means less ash covering the AC-Pm pore surface, resulting in more pores. As a result, it has a larger pore surface area and volume.

Table 3 Adsorption performance of activated carbons.

Activated carbons	N_2 (cm^3/g)	CO_2 (mmol/g)	Methylene blue (mg/g)
AC-Plt	75.252	1.554	1.215
AC-Pw	30.911	1.090	1.194

Table 4 Activated carbons performance for CO_2 adsorption.

Activated carbon precursors	Adsorption of CO_2 (mmol/g)	References
Rice husks	0.5 - 3.5	[42]
Sugarcane bagasse	1.66 - 4.8	[41]
Olive pomace	0.79 - 3.15	[43]
Polyacrylonitrile	0.3 - 1.2	[44]
Waste walnut shell	0.38 - 5.13	[45]

Activated carbon made from used brewed coffee for CO_2 absorption is very difficult to find, but many reports have been made from other raw materials. Several authors have reported CO_2 absorptions from various precursors (as shown in **Table 4**), and some of them were compared with the activated carbon prepared in this study. The adsorption of AC-Plt activated carbon on CO_2 was lower than that of N-doped activated carbons from sugarcane bagasse activated with KOH, as produced by Han *et al.* [41], which had a CO_2 adsorption capacity ranging from 1.66 to 4.8 mmol/g. However, the CO_2 adsorption capacities of AC-Plt and AC-Pw were superior to those of polyacrylonitrile activated carbon (0.3 - 1.2 mmol/g) [44], and comparable to those of activated carbon made from rice husks, activated with CO_2, and washed with K_2CO_3 produced by Li and Xiao [42], which had a CO_2 adsorption capacity in the range of 0.5 - 3.5 mmol/g under different temperature measurement conditions.

Conclusions

This research not only reduced the used brewed coffee, but it also resulted in products with added value. Two types of activated carbon were created using used brewed coffee as a precursor: Pelleted and powdered activated carbons using N_2 activator-physical activation method. This method is simple; there is no need for chemical agents, whose production process is more complicated and may have a negative impact on the environment if not handled properly. Pelleted activated carbon (AC-Plt) has better properties, such as lower ash (6.68 %), a higher surface area (105.857 m^2/g) and a lower pore volume (0.164 cm^3/g), than powdered activated carbon (AC-Pw). The use of organic binder in the manufacture of pellets causes pyrolysis during the activation process, resulting in the production of CO_2 gas, which also functions as a more reactive activator, which may explain why AC-Plt has a higher surface area and pore volume than AC-Pw. AC-Plt has a greater adsorption capacity for nitrogen (75,252 cm^3/g), CO_2 (1,554 mmol/g), and methylene blue (1,215 mg/g) than AC-Pw based on these properties. The research's weakness is that it is unclear whether the pressing process used to make pellets causes changes in the crystal structure of activated carbon. Additional tests, such as XRD, are required to comprehend the relationship between crystal structure, elemental ratio, interaction pattern with surface morphology, and gas adsorption mechanism. Aside from that, there are numerous intriguing aspects of activated carbon that need to be investigated, such as its life span, regeneration methods, and other potential applications.

Acknowledgements

I would like to express my gratitude to Udayana University's Research and Community Service Institute (LPPM) for funding this study, as well as to the Mechanical Engineering Department and the Faculty of Engineering at Udayana University, Indonesia for their assistance to this study.

References

[1] J Pallarés, A González-Cencerrado and I Arauzo. Production and characterization of activated carbon from barley straw by physical activation with carbon dioxide and steam. *Biomass Bioenerg.* 2018; **115**, 64-73.

[2] Y Mochizuki, J Bud, E Byambajav and N Tsubouchi. Influence of ammonia treatment on the CO_2 adsorption of activated carbon. *J. Environ. Chem. Eng.* 2022; **10**, 107273.
[3] X Ma, Y Wu, M Fang, B Liu, R Chen, R Shi, Q Wu, Z Zeng and L Li. In-situ activated ultramicroporous carbon materials derived from waste biomass for CO_2 capture and benzene adsorption. *Biomass Bioenerg.* 2022; **158**, 106353.
[4] L Spessato, VA Duarte, JM Fonseca, PA Arroyo and VC Almeida. Nitrogen-doped activated carbons with high performances for CO_2 adsorption. *J. CO2 Util*. 2022; **61**, 102013.
[5] E Surra, RPPL Ribeiro, T Santos, M Bernardo, JPB Mota, N Lapa and IAAC Esteves. Evaluation of activated carbons produced from maize cob waste for adsorption-based CO_2 separation and biogas upgrading. *J. Environ. Chem. Eng*. 2022; **10**, 107065.
[6] D Peredo-Mancilla, CM Ghimbeu, BN Ho, M Jeguirim, C Hort and D Bessieres. Comparative study of the CH_4/ CO_2 adsorption selectivity of activated carbons for biogas upgrading. *J. Environ. Chem. Eng*. 2019; **7**, 103368.
[7] C Wang, J Wang, W Wu, J Qian, S Song and Z Yue. Feasibility of activated carbon derived from anaerobic digester residues for supercapacitors. *J. Power Sourc.* 2018; **412**, 683-88.
[8] X Zhang, Y Wang, X Yu, J Tu, D Ruan and Z Qiao. High-performance discarded separator-based activated carbon for the application of supercapacitors. *J. Energ. Storage* 2021; **44**, 103378.
[9] P Arjunan, M Kouthaman, K Kannan, K Diwakar, V Priyanka, R Subadevi and M Sivakumar. Study on efficient electrode from electronic waste renewed carbon material for sodium battery applications. *J. Environ. Chem. Eng*. 2021; **9**, 105024.
[10] B Priyono, B Rifky, F Zahara and A Subhan. Enhancing performance of $Li_4Ti5012$ with addition of activated carbon from recycled pet waste as anode battery additives. *Evergreen* 2022; **9**, 563-70.
[11] AA Nuhu, ICP Omali and CO Clifford. Equilibrium adsorption studies of methylene blue onto caesalpinia pulcherrima husk-based activated carbon. *Chem. Sci. Int. J*. 2019; **26**, 1-11.
[12] P Ma, M Ma, J Wu, Y Qian, D Wu and X Zhang. The effect of plastic on performance of activated carbon and study on adsorption of methylene blue. *J. Mater. Res*. 2019; **34**, 3040-49.
[13] H Long, H Fei Lin, M Yan, Y Bai, X Tong, X Guo Kong and S Gang Li. Adsorption and diffusion characteristics of CH_4, CO_2, and N_2 in micropores and mesopores of bituminous coal: Molecular dynamics. *Fuel* 2021; **292**, 120268.
[14] SM Wang, PC Wu, JW Fu and QY Yang. Heteroatom-doped porous carbon microspheres with ultramicropores for efficient CH_4/N_2 separation with ultra-high CH_4 uptake. *Separ. Purif. Tech*. 2021; **274**, 119121.
[15] AF Ridassepri, AF Ridassepri, F Rahmawati, KR Heliani, J Miyawaki and AT Wijayanta. Activated carbon from bagasse and its application for water vapor adsorption. *Evergreen* 2020, **7**, 409-16.
[16] K Thu, T Miyazaki, K Nakabayashi, J Miyawaki and AT Wij. Highly microporous activated carbon from acorn nutshells and its performance in water vapor adsorption. *Evergreen* 2021; **8**, 249-54.
[17] M Hamid, MH Mahmood, M Sultan and T Miyazaki. Study on water-vapor adsorption onto polymer and carbon-based adsorbents for air- conditioning applications. *Evergreen* 2019; **6**, 215-24.
[18] W Qian, M Hossein and Y Sun. Investigation on the effect of functionalization of single-walled carbon nanotubes on the mechanical properties of epoxy glass composites: Experimental and molecular dynamics simulation. *J. Mater. Res. Tech*. 2021; **12**, 1931-45.
[19] P Talebizadehsardari, A Shahsavar, D Toghraie and P Barnoon. An experimental investigation for study the rheological behavior of water-carbon nanotube/magnetite nanofluid subjected to a magnetic field. *Phys. Stat. Mech. Appl.* 2019; **534**, 122129.
[20] R Maleki, HH Afrouzi, M Hosseini, D Toghraie and S Rostami. Molecular dynamics simulation of Doxorubicin loading with N-isopropyl acrylamide carbon nanotube in a drug delivery system. *Comput. Meth. Programs Biomed*. 2019; **184**, 105303.
[21] EH Sujiono, D Zabrian, Zurnansyah, Mulyati, V Zharvan, Samnur and NA Humairah. Fabrication and characterization of coconut shell activated carbon using variation chemical activation for wastewater treatment application. *Results Chem*. 2022; **4**, 100291.
[22] W Widanarto, S Irma, S Krishna, C Kurniawan, Handoko and M Alaydrus. Improved microwave adsorption traits of coconut shells-derived activated carbon. *Diam. Relat. Mater.* 2022; **126**, 109059.
[23] J Han, L Zhang, B Zhao, L Qin, Y Wang and F Xing. The N-doped activated carbon derived from sugarcane bagasse for CO_2 adsorption. *Ind. Crop. Prod*. 2018; **128**, 290-7.
[24] DNK Putra Negara, TGT Nindhia, Lusiana, IM Astika and CIPK Kencanawati. Development and characterization of activated carbons derived from lignocellulosic material. *Mater. Sci. Forum* 2020; **988**, 80-6.

[25] SL Ezung, M Baruah, A Supong, S Sharma and D Sinha. Experimental and theoretical insight into the adsorption of 2, 4-dichlorophenol on low-cost bamboo sheath activated carbon. *Sustain. Chem. Pharm*. 2022; **26**, 100643.
[26] IM Astika, DNK Putra Negara, CIPK Kencanawati, TGT Nindhia and F Hidajat. Proximate and morphology properties of swat bamboo activated carbon carburized under different carbonization temperature. *IOP Conf. Ser. Mater. Sci. Eng.* 2019; **539**, 012010.
[27] S Wang, YR Lee, Y Won, H Kim, SE Jeong, B Wook Hwang, AR Cho, JY Kim, YC Park, H Nam, DH Lee, H Kim and SH Jo. Development of high-performance adsorbent using KOH-impregnated rice husk-based activated carbon for indoor CO_2 adsorption. *Chem. Eng. J*. 2022; **437**, 135378.
[28] ER Raut, MA Bedmohata and AR Chaudhari. Comparative study of preparation and characterization of activated carbon obtained from sugarcane bagasse and rice husk by using H_3PO_4 and $ZnCl_2$. *Mater. Today Proc*. 2022; **66**, 1875-84.
[29] A Mukherjee, JA Okolie, C Niu and AK Dalai. Techno - economic analysis of activated carbon production from spent coffee grounds: Comparative evaluation of different production routes. *Energ. Convers. Manag*. X 2022; **14**, 100218.
[30] R Hossain, RK Nekouei, I Mansuri and V Sahajwalla. In-situ O/N-heteroatom enriched activated carbon by sustainable thermal transformation of waste coffee grounds for supercapacitor material. *J. Energ. Storage* 2021; **33**, 102113.
[31] Y Wibisono, A Amanah, A Sukoyo, F Anugroho and E Kurniati. Activated carbon loaded mixed matrix membranes extracted from oil palm empty fruit bunches for vehicle exhaust gas adsorbers. *Evergreen* 2021; **8**, 593-600.
[32] R Muhammad and S Adityosulindro. Biosorption of brilliant green dye from synthetic wastewater by modified wild algae biomass. *Evergreen* 2022; **9**, 133-40.
[33] H Liu, C Cheng and H Wu. Sustainable utilization of wetland biomass for activated carbon production: A review on recent advances in modification and activation methods. *Sci. Total Environ*. 2021; **790**, 148214.
[34] DNK Putra Negara, TGT Nindhia, M Sucipta, IW Surata, KS Astrawan and IPH Wangsa. Simultaneous adsorption of motorcycle emissions through bamboo-activated carbon. *Int. J. Glob. Energ. Issues* 2021; **43**, 199-210.
[35] M Saberian, J Li, A Donnoli, E Bonderenko, P Oliva, B Gill, S Lockrey and R Siddique. Recycling of spent coffee grounds in construction materials: A review. *J. Clean. Prod*. 2021; **289**, 125837.
[36] OOD Afolabi, M Sohail and Y Cheng. Optimisation and characterisation of hydrochar production from spent coffee grounds by hydrothermal carbonization. *Renew. Energ.* 2020; **147**, 1380-91.
[37] DN Mengesha, MW Abebe, R Appiah-ntiamoah and H Kim. Ground coffee waste-derived carbon for adsorptive removal of caffeine: Effect of surface chemistry and porous structure. *Sci. Total Environ*. 2022; **818**, 151669.
[38] L Hadebe, Z Cele and B Gumbi. Proceedings properties of porous carbon electrode material derived from biomass of coffee waste grounds for capacitive deionization. *Mater. Today Proc.* 2022; **56**, 2178-83.
[39] FM Ferraz and Q Yuan. Organic matter removal from landfill leachate by adsorption using spent coffee grounds activated carbon. *Sustain. Mater. Tech.* 2020; **23**, e00141.
[40] F Mbarki, T Selmi, A Kesraoui and M Seffen. Low-cost activated carbon preparation from corn stigmata fibers chemically activated using H_3PO_4, $ZnCl_2$ and KOH: Study of methylene blue adsorption, stochastic isotherm and fractal kinetic. *Ind. Crop. Prod.* 2022: **178**, 114546.
[41] J Han, L Zhang, B Zhao, L Qin, Y Wang and F Xing. The N-doped activated carbon derived from sugarcane bagasse for CO_2 adsorption. *Ind. Crop Prod*. 2019; **128**, 290-97.
[42] M Li and R Xiao. Preparation of a dual pore structure activated carbon from rice husk char as an adsorbent for CO_2 capture. *Fuel Process. Tech*. 2019; **186**, 35-9.
[43] K Kie, M Bosacka and B Michalkiewicz. Thermochemical conversion of lignocellulosic biomass - olive pomace - into activated biocarbon for CO_2 adsorption. *Ind. Crop. Prod*. 2022; **187**, 115416.
[44] J Singh, S Basu and H Bhunia. Dynamic CO_2 adsorption on activated carbon adsorbents synthesized from polyacrylonitrile (PAN): Kinetic and isotherm studies. *Microporous Mesoporous Mater.* 2019; **280**, 357-66.
[45] J Shi, H Cui, J Xu, N Yan and S You. Synthesis of N-doped hierarchically ordered micro-mesoporous carbons for CO_2 adsorption. *J. CO2 Util*. 2022; **62**, 102081.